Published in final edited form as:
Cell Tissue Res. 2008 October ; 334(1): 55–65. doi:10.1007/s00441-008-0623-7.

Endothelial cell suppression of peripheral blood mononuclear cell trafficking in vitro during acute exposure to feline immunodeficiency virus

Lola C. Hudson,
Department of Molecular Biomedical Sciences, College of Veterinary Medicine, 4700 Hillsborough Street, Raleigh, NC 27606, USA

Mary B. Tompkins, and
Immunology Program, North Carolina State University, Raleigh, NC 27606, USA

Rick B. Meeker
Department of Neurology, School of Medicine, University of North Carolina, Chapel Hill, NC 27599, USA

Abstract

Trafficking of peripheral blood mononuclear cells (PBMCs) into the brain is a critical step in the initiation of human immunodeficiency virus (HIV)-associated central nervous system disease. To examine potential factors that control trafficking during the earliest stages of infection, PBMC transmigration across a cultured feline brain endothelial cell (BECs) monolayer was measured after selective exposure of various cell types to feline immunodeficiency virus (FIV). Infection of the PBMCs with FIV increased the trafficking of monocytes and CD4 and CD8 T cells. Additional exposure of the BECs to FIV suppressed mean monocyte, CD4 T cell, and CD8 T cell trafficking. B cell trafficking was unaltered by these changing conditions. Subsequent exposure of astrocytes or microglia to FIV altered transmigration of different PBMC subsets in different ways. Treated microglia compared with treated astrocytes decreased monocyte transmigration, whereas B cell transmigration was increased significantly. When both astrocytes and microglia were exposed to FIV, an increase in CD8 T cell transmigration relative to BECs alone, to BECs plus astrocytes, or to BECs plus microglia was demonstrated. Thus, initial exposure of PBMCs to FIV is sufficient to induce a general increase in trafficking, whereas initial exposure of endothelial cells to FIV tends to down-regulate this effect. Selectivity of trafficking of specific PBMC subsets is apparent only after exposure of cells of the central nervous system to FIV in co-culture with the endothelium.

Keywords

HIV; Astrocytes; Microglia; Monocyte; Tcell; Feline

Introduction

Lentiviruses such as human immunodeficiency virus (HIV) rapidly penetrate the central nervous system (CNS). Previous publications indicate that transmigrating monocytes and perhaps T cells are major vehicles for viral trafficking across the brain endothelium (Kim et al. 2004; Nottet et al. 1996; Persidsky et al. 1997; Petito et al. 2003; Williams and Hickey

L. C. Hudson lola_hudson@ncsu.edu.

2002). Once viruses enter the brain, they are partially protected from anti-retroviral therapy making it difficult to eradicate them (McGee et al. 2006; Clements et al. 2005). Because of this protected status of virus in the brain, much effort has been devoted to understanding the mechanisms that control virus entry in order to develop strategies to reduce or eliminate CNS infection. Some of these studies have focused on in vitro models utilizing brain microvascular endothelial cells cultured in various combinations with microglia and sometimes astrocytes (Nottet et al. 1996; Persidsky 1999). These studies have also examined the role that especially microglia play in the control of monocyte trafficking and cell-associated virus trafficking into the CNS (Gray et al. 1992; Koenig et al. 1986; Zheng and Gendelman 1997; Nottet et al. 1996; Persidsky 1999). Results from these studies have shown that activated monocytes traffick across brain endothelium at increased rates, although the trafficking is independent of infection (Nottet et al. 1996). Infection of microglia with HIV also results in increased monocyte trafficking, which again is independent of infection (Persidsky et al. 1997). More recent data from simian immunodeficiency virus (SIV) and HIV infections have suggested that CD16 and CD163 monocytes may selectively traffick into the brain (Bissel et al. 2006; Roberts et al. 2004). The role of other mononuclear cells, viz., CD4 T cells, CD8 T cells, and B cells, and of other CNS cells in immunodeficiency virus infection of the CNS has not been well studied. An analysis of the relative contribution of microglia and astrocytes with and without feline immunodeficiency virus (FIV) treatment has demonstrated that the trafficking of uninfected peripheral blood mononuclear cells (PBMCs) is highly dependent on the presence of astrocytes (Hudson et al. 2005). Untreated monocytes, CD4 T cells, CD8 T cells, and B cells all move most efficiently across brain endothelium when astrocytes are present in a transwell culture system. Untreated microglia co-cultured with the astrocytes always reduce the level of trafficking suggesting that these cells exert inhibitory control over the astrocytes thereby making the barrier less permissive to trafficking. However, when FIV is added to the cultures of CNS cells, this ability of microglia to restrict trafficking, in particular monocyte trafficking, is lost. Whereas these studies have clearly shown that cells within the brain parenchyma exert significant control over trafficking, questions remained regarding the interactions between infected PBMCs and the cells of the brain endothelium and parenchyma. In vivo, the PBMCs and peripheral lymphoid tissue are the first infected (English et al. 1993; Strand 1982) followed by changes at the brain endothelium, even without productive infection (Harper et al. 1986). Later in the course of the disease, the brain parenchyma exhibits evidence of infection (Wiley et al. 1986; Liu et al. 2006a, b). Animal models have shown that the initial penetration of virus into the brain is cleared and is then followed by a more persistent and perhaps permanent entry (Liu et al. 2006a, b). Definition of the evolving mechanisms of virus entry into the nervous system is crucial to the development of therapeutic strategies to eliminate infection of the CNS. Natural immunodeficiency virus (HIV/SIV/FIV) infections of the nervous system frequently include both virus in circulating PBMCs and virus exposure of CNS cells. Therefore, the experiments in this study have assessed the role of virus interactions with PBMCs, endothelial cells, astrocytes, and microglia and, in particular, any interactions that might support early virus penetration into the CNS.

Materials and methods

Cultured cells

The source of fetal tissue, isolation methods of CNS cells and PBMCs, and characterization of cells were as previously described in detail (Hudson et al. 2005). Briefly, the brains of deceased feline fetuses were removed, washed, and cleaned of meninges. The cerebral hemispheres were minced and dissociated enzymatically for brain endothelial cells (BECs) or astrocytes, by using previously published isolation methods (Sapatino et al. 1993; Dow et

al. 1992) or were ground through a wire mesh by using a long established method for microglia. For the latter, nonadherent microglia were collected from the resulting mixed culture. The purity of these primary cultures was determined by using specific cell markers and ranged from >80% for BECs to >95% for astrocytes and microglia. BECs were subcultured for a maximum of six passages, and cells from each passage were frozen for later use. Astrocytes were subcultured a maximum of once, and microglia were not subcultured.

Cell culture in transwell insert system

Diverse combinations of BECs, astrocytes, and microglia were used to evaluate the role of individual cell types to the trafficking of PBMCs with and without virus treatment. The various configurations and number of replicates analyzed are summarized in Table 1. BECs (and ultimately PBMCs) were present in the upper chamber of transwell inserts for all experiments and combined with treated astrocytes and/or microglia in the lower chamber to complete the transwell system. PBMCs were added to the upper chamber with the BEC monolayer 24 h after the transwell system was completed (see Fig. 1). Each cell component of the transwell system was then exposed to FIV in order to examine each interaction.

Endothelial cells were seeded at 5×10^5/insert onto a transwell insert membrane coated with collagen (Biocoat, Becton Dickenson, Bedford, Mass.) and containing 3-μm pores. BECs were allowed to grow to confluence, which generally took 2–3 days. For experiments that would include astrocytes or microglia, the appropriate cell type(s) was seeded at 1×10^5 into the lower chamber without virus treatment, and the newly seeded BEC inserts were placed into the well. This would allow exposure of BECs to any secreted factors normally produced by the accessory cells. Then, in separate plates, astrocytes and microglia were seeded at the same density into the well (which would become the lower chamber) for 2 days. On day 2, astrocytes or microglia (without inserts) were treated with FIV for 24 h (also see below). The astrocytes or microglia werewashed three times, and the inserts with confluent untreated BECs were transferred to the treated wells. Experiments utilizing BECs as the only CNS cell also involved this FIV treatment onto the confluent cells for 24 h. The BECs were washed three times. After the exposure of BECs, astrocytes, or microglia to the virus and the wash steps, 1×10^5 PBMCs were added to the upper chamber of each well. For all experiments, PBMCs that were isolated on Percoll gradient were stimulated overnight with 2 μg/ml of Concanavalin A (conA) as previously described (Hudson et al. 2005). For experiments utilizing virus-treated PBMCs, these cells were also treated with the same strain of FIV for 24 h. PBMCs were washed three times and were labeled with 5 μM Cell Tracker Orange (Molecular Probes, Invitrogen, Carlsbad, Calif.). They were then added to the upper chamber of the cell culture inserts for 24 h.

Treatment with FIV

To simulate the earliest stages of infection with regard to the CNS, treatment of PBMCs with 1×10^4 $TCID_{50}$ $NCSU_1$-FIV (English et al. 1993)/1×10^5 PBMCs (multiplicity of infection [MOI] of 0.1) was performed for 24 h, with the PBMCs subsequently being referred to as infected or uninfected. The provirus copy number was determined by polymerase chain reaction (PCR; see below). This was followed by wash steps, labeling with 5 μM Cell Tracker Orange (Molecular Probes) as recommended by the manufacturer, and coculture of PBMCs with untreated BECs for 24 h. PBMC adherence to the BEC monolayer and transmigration of different PBMC subsets into the lower chamber of the transwell insert were then determined (see below). This experiment was followed by determination of the interaction of virus-treated BECs (50 μl 1×10^4 $TCID_{50}$/100 μl $NCSU_1$ strain of FIV) for 24 h, three washes of the monolayer, and coculture with virus-treated

PBMCs (as above) for 24 h. Controls included untreated PBMCs with untreated BECs, and treated BECs with untreated PBMCs.

Experiments exploring the role of virus-exposed astrocytes and microglia were then performed. On day 3 after seeding, astrocytes or microglia (without the BEC insert; see Fig. 1b) were exposed to 50 μl 1×10^4 $TCID_{50}$/100 μl $NCSU_1$ strain of FIV for 24 h. After the cells had been washed, an insert with a confluent monolayer of BECs was transferred into the well, and virus-infected labeled PBMCs (as above) were added to the upper chamber for 24 h. Controls of these experiments used the same density of cells and time points, but the FIV treatment of the CNS cells and PBMCs was substituted with fresh medium (Table 1).

Earlier studies have determined that brain endothelial cells do not develop a productive infection with immunodeficiency virus when non-cell-adapted strains are used, such as those here (Steffan et al. 1994). Additionally, astrocytes and microglia are known not to develop productive infections within 24 h (Dow et al. 1992; Meeker et al. 1999). Therefore, these cells are referred to as virus exposed below.

Adherence of PBMCs

After 24-h coculture, the inserts were gently washed to remove any non-adhered PBMCs, and the insert membranes were removed and mounted onto slides in a manner to allow the counting of PBMCs adhered to the upper surface of the endothelial cells (simulating the vascular lumen). Fluorescent PBMCs adhered to the superficial surface of the BEC monolayer were counted in five independent fields (field=0.2515 mm^2) for each membrane by using an inverted microscope equipped with a digital charge-coupled device camera and Metamorph imaging software (Universal Imaging, Westchester, Pa.). Fluorescent objects were counted after filtration by size to restrict measurement of objects with the size of white blood cells. Counts were averaged within each insert to provide a single value for each insert and then averaged across inserts.

Immunocytochemistry

The medium from the lower chambers of configurations that included transmigrated PBMCs was collected, evenly divided, and cytospun as described previously (Hudson et al. 2005). The cells were then immunostained for CD3, CD4, CD8, B cell, or monocyte markers (see Table 2) and manually counted.

Western blot analysis

Brain endothelial cells were grown in 25-cm^2 flasks until confluent. Fresh medium containing either no additional materials or FIVat an MOI of 0.5 was added to these cultures for 24 h. Cells were sonicated in buffer (50 mM TRIS-HCl, 150 mM NaCl, 1 mM EDTA, pH 8.0) with freshly added protease inhibitors (final concentrations: 50 μg/ml pepstatin A, 50 μg/ml chymostatin, 50 μg/ml leupeptin, 100 μg/ml aprotinin). Protein concentrations were determined by Bradford assay. Positive control, untreated sample, and treated sample wells were loaded with 45 μg protein in SDS buffer. Boiled samples were subjected to electrophoresis in a 7.5% polyacrylamide gel and then transferred to polyvinylidene difluoride (PVDF) membrane overnight at 4°C and 40 mV. The membrane was blocked in 5% skim milk buffer for 1 h, incubated with primary antibody for intracellular adhesion molecule 1 (ICAM1), ICAM2, and vascular cell adhesion molecule (VCAM; see Table 2) for 1 h at room temperature, and then incubated with horseradish peroxidase (HRP)-conjugated secondary antibody for 1 h at room temperature. Peroxidase activity was detected by use of chemiluminescence. Bands were imaged by using a bioimaging system and Labworks software (UVP, Upland, Calif.). The membranes were then stripped by using a commercial product (Santa Cruz Biotechnology) and reprobed with actin antibody and

appropriate HRP-conjugated secondary antibody as a loading control (Table 2). The actin bands were imaged as above. For the resulting figure, blot images were optimized by adjusting the contrast to view bands, and pertinent sample lanes were digitally placed adjacent to each other. Bands were measured by using densitometric software (Labworks software). Densitometry values were then normalized to the actin untreated control for each adhesion molecule.

Detection of provirus by PCR

Blood was collected from SPF cats that were negative for FIV infection by antibody test, and negative by reverse transcriptase PCR of both cerebrospinal fluid (CSF) and plasma (Liu et al. 2006a, b). After Percoll separation of PBMCs, the cells were counted, stimulated with conA as above, and exposed to FIV at an MOI of 0.1 for 24 h as for the culture insert experiments. After the exposed cells were washed three times, the PBMCs were collected, and 1×10^6 PBMCs were processed for DNA with a kit (Qiagen, Valencia, Calif.). Real time PCR analysis for FIV provirus was performed with previously published primers and labeled probe (English et al. 1993; Liu et al. 2006a, b). A standard curve was generated from a pcDNA3.1-gag plasmid sample (Liu et al. 2006a, b).

Statistical analysis

Data on PBMC adherence and transmigration was analyzed by analysis of variance with Tukey's post-hoc paired comparisons (GraphPad Prism software or Minitab software). The absolute numbers of transmigrating PBMC subsets was variable from run to run, resulting in a non-normal distribution in most instances. Consequently, the Mann-Whitney test was also used to evaluate changes in paired data.

Results

Infection of PBMCs

Acute exposure of PBMCs to $NCSU_1$-FIV resulted in detectable provirus (87 copies per 10^6 PBMCs compared with 0 copies for unexposed PBMCs) in 24 h by using real time PCR. The exposure level (MOI of 0.1) simulated values reported previously for in vivo circulating infected feline PBMCs (Dean et al. 1996).

Effect of FIV exposure to PBMCs and BECs on adhesion and transmigration

To assess possible changes in trafficking as virus exposure passes from blood to include endothelium, PBMCs were infected with FIV and then co-cultured with either untreated or treated endothelial monolayer. Treated endothelial cells in the upper chamber were exposed to FIV continuously for the 24-h period prior to the initiation of trafficking in order to mimic the exposed brain vasculature. The control group for this series of experiments involved untreated endothelial cells and PBMCs.

Acute infection of PBMCs with FIV for 24 h did not alter the adherence of the PBMCs to the surface of untreated endothelial cells. An average of 11.2 uninfected PBMCs/field tightly adhered to the endothelial surface versus 12.4 infected PBMCs/field (Fig. 2a). Independent exposure of the endothelial cells with FIV also failed to influence the adherence of infected PBMCs (12.1 PBMCs/field), although exposed BECs with uninfected PBMCs showed a significant decrease in adhered PBMCs (3.2 PBMCs/field).

Constitutive expression of VCAM in BECs was absent to very low (Fig. 3). There was a non-significant increase in VCAM expression after FIV treatment. ICAM1 expression in BECs was constitutively low and decreased about 50% on exposure to FIV compared with the untreated level. ICAM2 constitutive levels were more robust than either VCAM or

ICAM1, but expression in endothelial cells decreased about 50% with exposure to FIV, a finding consistent with the decreased PBMC adherence to virus exposed BECs seen in Fig. 2a.

In the absence of FIV infection, T cells transmigrated at the lowest rate, whereas monocytes transmigrated at a higher rate and B cells at the highest rate (Hudson et al. 2005). Infection of the PBMCs influenced transmigration in a cell-specific fashion. The transmigration of monocytes and CD4 T cells was increased after exposure of the isolated PBMCs to FIV (Fig. 4, light gray bar). This increase was significant for the CD4 T cells ($P<0.05$). When the infected PBMCs were added to brain endothelial cells that were also exposed to FIV for 24 h, transmigration of monocytes and CD4 T cells was greatly diminished (Fig. 4, dark gray bar). However, it was a significant decrease only for the monocyte transmigration ($P<0.05$). Transmigration of CD8 cells was also diminished under the same conditions but was very low under all conditions. B cells transmigration did not change significantly after infection of the PBMCs or endothelial cells. The combination of FIV exposed BECs with unexposed PBMCs resulted in the lowest transmigration of all PBMC subsets.

Effect of FIV exposure to astrocytes and microglia on adhesion and transmigration of infected PBMCs

To assess possible changes in trafficking as virus exposure moves into the CNS, astrocytes and/or microglia were exposed to FIV and then co-cultured with BECs. The infected PBMCs were then added to the endothelial monolayer with astrocytes, microglia, or a combination of astrocytes and microglia present in the lower chamber of cell culture inserts. In each case, cells in the lower chamber were exposed to FIV continuously for the 24-h period prior to the initiation of trafficking in order to mimic the exposed brain parenchyma. Controls for this series of experiments involved untreated endothelial cells, astrocytes, microglia, and PBMCs.

Astrocyte and microglial effects on PBMC adherence—The presence of FIV-exposed astrocytes in the bottom chamber of cell culture inserts significantly increased the adherence of infected PBMCs to BECs, whereas FIV-exposed microglia alone had little effect (Fig. 2b). When both astrocytes and microglia were present, the effect of the astrocytes was slightly suppressed (Fig. 2b) but did not reach significance. These configurations when compared with the same combination of untreated cells did not have an altered adherence.

Astrocyte and microglial effects on transmigration of monocytes—When PBMCs and astrocytes or microglia were exposed to FIV, the transmigration of separate PBMC subsets was variable. This addition of FIV treatment resulted in a lowered mean transmigration of monocytes in the presence of astrocytes and/or microglia compared with these untreated configurations with untreated PBMCs. As summarized in Fig. 5a, the FIV-exposed astrocytes increased the level of trafficking of the monocyte subset within the FIV-infected PBMCs. However, FIV-exposed microglia alone significantly suppressed monocyte trafficking by 87%. FIV-exposure of microglia in combination with astrocytes suppressed monocyte trafficking by 67% in comparison with FIV-exposed astrocytes alone indicating that the microglia have an inhibitory effect on monocyte transmigration. Additionally, the mean transmigration of monocytes, when FIV-infected, was always less than the mean transmigration of monocytes that were uninfected.

Astrocyte and microglial effects on transmigration of CD4 T cells—There was a trend for trafficking of CD4 T cells (summarized in Fig. 5b) to be facilitated in the presence of FIV-exposed astrocytes and suppressed by FIV-exposed microglia. When both FIV-

exposed astrocytes and microglia were present, the largest mean number of CD4 T cells was trafficked, but this increase was not statistically significant.

Astrocyte and microglial effects on transmigration of CD8 T cells—Relatively few CD8 T cell transmigrated across the endothelium. The results (summarized in Fig. 5c) indicated that the transmigration was unaffected by the addition of FIV-exposed astrocytes or of FIV-exposed microglia alone. However, the combination of astrocytes and microglia with FIV significantly increased the trafficking of the CD8 T cells suggesting a synergistic effect of these cells.

Astrocyte and microglial effects on transmigration of B cells—The number of B cells that migrated from the upper chamber, across the endothelium, and into the lower chamber significantly increased in the presence of FIV-treated astrocytes and FIV-treated PBMCs compared with endothelial cells alone (Fig. 5d). A still greater and significant increase was seen in the presence of FIV-exposed microglia. When both astrocytes and microglia were present and exposed to FIV, the number of transmigrated B cells was equivalent to the number seen with astrocytes alone. The difference in mean transmigration between FIV-treated cells and untreated cells in the presence of endothelial cells and astrocytes was significant for B cells.

Discussion

When the host organism is infected with a lentivirus such as HIV, SIV, or FIV, a sequence of events gives rise to the distribution of the virus throughout the body. HIV is most commonly spread via unprotected sexual intercourse and use of contaminated needles during intravenous drug use (Janeway et al. 2005; Klevens et al. 1999; Quinn 1995). For animal immunodeficiency viruses, most natural infections are communicated via sexual transmission or bite wounds contaminated with infected saliva (Novotney et al. 1990; Gunn-Moore et al. 1996; Beebe et al. 1992; Pedersen and Barlough 1991). These common methods of immunodeficiency virus exposure afford rapid access to the monocytes and lymphocytes of the blood stream and dissemination to other organ systems, particularly lymphoid tissue (Dianzani et al. 1996; Pantaleo et al. 1991). Most data concerning the early stages of infection support the idea both that the PBMCs are infected, and that plasma viremia is established prior to virus entry into the brain parenchyma and CSF, although the temporal relationship is apparently close (Liu et al. 2006a, b).

The entire process of trafficking cells through an endothelium requires four basic steps: rolling, adhesion (or arrest), transmigration (or diapedesis), and migration through tissue. These are separate steps with different control mechanisms. Adherence is generally accepted as being a rate-limiting step for later transmigration to occur, and relatively low adherence is followed by relatively low transmigration. However, the converse is not necessarily true, e.g., increased adherence is not necessarily followed by increased transmigration because mechanisms for the different steps are not locked together, as is supported by the data in this report. Additionally, our time points have been chosen to optimize findings for transmigration. As a result, the peak in adherence of PBMCs is possibly past, although the data are still statistically significant.

Influence of BECs on trafficking of infected PBMCs

The interactions between virus, PBMCs, and the CNS triad of BECs, astrocytes, and microglia are crucial to the development of CNS disease but are not well understood. In the current study, the interactions of FIV-infected PBMCs with BECs were first assessed under conditions that simulate the initial trafficking of cells, potentially containing virus, into the

naive CNS. To accomplish this, PBMCs that were acutely infected with FIV were seeded into transwell inserts containing a monolayer of unexposed BECs. This represented the very earliest stages of infection, even prior to the development of a significant plasma viremia. A separate set of cultures was used in which both the PBMCs and BECs were exposed to virus, thereby simulating the conditions present during early plasma viremia. Under both of these conditions, adherence of PBMCs remained unchanged. This suggests that, during in vivo immunodeficiency virus infection when uninfected PBMCs constitute the largest percentage of circulating PBMCs (Dean et al. 1996), the uninfected PBMCs are less likely to adhere to a virus-exposed endothelium. Moreover, cells that do not adhere to the endothelium are not available for the subsequent steps of transmigration.

Under the condition of treated PBMCs and untreated BECS, monocytes or CD4 T cells demonstrate the greatest increase in mean transmigration. These findings suggest that the trafficking of CD4 T cells and monocytes is facilitated during the initial stages of infection, before exposure of the endothelial cells to the virus. The trafficking of B cells and CD8 T cells under this condition is essentially unaltered.

This early spike in T cell and monocyte trafficking may serve as an explanation for the rapid development of infection both peripherally and centrally, as reported in an unfortunate case of iatrogenic intravenous HIV exposure of an HIV-negative individual (Davis et al. 1992). Despite treatment with zidovudine for 3 days within 45 min of exposure, this individual was positive for provirus by PCR within 8 days peripherally and at 15 days post-exposure in brain tissue.

As the plasma viremia develops and the brain endothelial cells are exposed to cell-free virus, the trafficking of monocytes then decreases significantly. A substantial reduction in infected or uninfected CD4 T cell trafficking is also seen with no effect on CD8 T cells or B cells. This observation suggests that the acute effect of FIV exposure on the endothelium is preferentially to suppress the trafficking of CD4 T cells and monocytes. The reduction in ICAM1 and ICAM2 expression supports this conclusion. Thus, at the early stages of infection, mechanisms may exist first to increase and then to limit the amount of immune cell trafficking. These results indicate that acute exposure to lentiviruses does not damage the blood-brain barrier or promote trafficking via a leaky barrier (Boven et al. 2000; Annunziata 2003; Dallasta et al. 1999). Two possible outcomes might be predicted from these observations. First, a down-regulation of early immune cell trafficking by FIV may restrict the influx of infected cells and may explain the rapid clearance of virus and immune cells from the CNS after the initial peak of virus in the plasma and CSF (Zink et al. 1997; Ryan et al. 2003). On the other hand, immune cell trafficking important for viral clearance may be suppressed during this early critical period after the virus gains access to the CNS. As the infection progresses, other factors may come into play that override this inhibitory effect, allowing for a gradual infiltration of monocytes and/or T cells with increased virus exposure to astrocytes and microglia, as discussed below. If intrinsic mechanisms are present that can restrict the trafficking of immune cells across the brain endothelium, then we might be able to exploit these processes for therapeutic applications.

Influence of astrocytes and microglia on trafficking of infected PBMCs

An earlier study has found that the presence of astrocytes and microglia greatly influences the adherence and transmigration of uninfected PBMCs (Hudson et al. 2005). The current study comparing treated and untreated PBMCs (Fig. 5) also shows that astrocytes encourage PBMC adherence, whereas microglia tend to reverse this effect. These changes are independent of virus exposure.

The effect of the astrocytes on the transmigration of PBMC subsets (Fig. 5), however, is less robust with treated PBMCs than with untreated PBMCs. The astrocytes effect is perhaps being overridden by the infection of the PBMCs. Monocytes show a relatively increased level of transmigration in the presence of treated astrocytes, whereas the presence of microglia suppresses this trafficking. An inhibitory effect of microglia on CD4 T cells has also been seen, although the microglia tend to support the trafficking of CD8 T cells and B cells. Previous studies have indicated that monocyte activation in the presence of untreated astrocytes is sufficient to promote trafficking (Persidsky et al. 1997). In a similar study, Persidsky et al. (1999) have demonstrated that the presence of infected microglia encourages the trafficking of uninfected monocytes in part because of the increased secretion of MCP-1. A robust secretion of MCP-1 from astrocytes is consistent with their positive role in trafficking as seen in this and related studies (Persidsky et al. 1999; Hudson et al. 2005). The precise role of microglia is not as clear. The studies by Persidsky et al. (1999) and Hudson et al. (2005) both show that infected microglia support monocyte trafficking. However, in the latter study, increases in trafficking appear to be attributable to the loss of an inhibitory action seen in the uninfected microglia. This concept is supported in the present study, although the impact of the microglia appears to be partially overridden by infection of the PBMCs. Thus, direct activation of the monocytes by FIV may encourage higher levels of trafficking independent of contributions from the parenchymal cells. The synergistic effect of astrocytes and microglia on CD8 T cell trafficking suggests that these cells may be primarily under the control of factors derived from the brain parenchyma. This observation could provide an important functional distinction between the trafficking of CD4 and CD8 T cells and may provide some understanding of the accumulation of CD8 T cells in the brain of HIV patients over time (Petito et al. 2003).

The addition of either treated astrocytes or microglia to the cultures facilitates B cell transmigration. As in the previous experiments, an antagonistic relationship between the independent effects of the astrocytes and the microglia is often seen.

Overall, these observations suggest a sequence of events during the early stages of infection. Acutely infected/activated blood cells initially move into the CNS followed by the suppression of trafficking as the plasma viral load rises. A resurgence of trafficking subsequently occurs as parenchymal infection begins to reverse some of the natural inhibitory processes. This scenario may partially explain the rapid appearance and disappearance of virus after initial infection and the paucity of pathologic changes that can be detected by sundry methods within CNS tissue during acute immunodeficiency infection. Indeed, during acute or asymptomatic stages of infection, these interactions may effectively reduce the opportunity for CNS invasion via the blood-brain interface.

Acknowledgments

This investigation was supported by funds from NIH (MH63646 and AI47749) and by the state of North Carolina.

References

Annunziata P. Blood-brain barrier changes during invasion of the central nervous system by HIV-1. Old and new insights into the mechanism. J Neurol. 2003; 250:901–906. [PubMed: 12928906]

Beebe A, Gluckstern T, George J, Pedersen N, Dandekar S. Detection of feline immunodeficiency virus infection in bone marrow of cats. Vet Immunol Immunopathol. 1992; 35:37–49. [PubMed: 1337401]

Bissel SJ, Wang G, Trichel AM, Murphey-Corb M, Wiley CA. Longitudinal analysis of activation markers on monocyte subsets during the development of simian immunodeficiency virus encephalitis. J Neuroimmunol. 2006; 177:85–98. [PubMed: 16797085]

Boven LA, Middel J, Verhoef J, De Groot CJ, Nottet HS. Monocyte infiltration is highly associated with loss of the tight junction protein zonula occludens in HIV-1-associated dementia. Neuropathol Appl Neurobiol. 2000; 26:356–360. [PubMed: 10931369]

Clements JE, Li M, Gama L, Bullock B, Carruth LM, Mankowski JL, Zink MC. The central nervous system is a viral reservoir in simian immunodeficiency virus-infected macaques on combined antiretroviral therapy: a model for human immunodeficiency virus patients on highly active antiretroviral therapy. J Neurovirol. 2005; 11:180–189. [PubMed: 16036796]

Dallasta LM, Pisarov LA, Esplen JE, Werley JV, Moses AV, Nelson JA, Achim CL. Blood-brain barrier tight junction disruption in human immunodeficiency virus-1 encephalitis. Am J Pathol. 1999; 155:1915–1927. [PubMed: 10595922]

Davis LE, Helle BL, Miller VE, Palmer DL, Llewellyn AL, Merlin TL, Young SA, Mills RG, Wachsman W, Wiley CA. Early viral brain invasion in iatrogenic human immunodeficiency virus infection. Neurology. 1992; 42:1736–1739. [PubMed: 1513462]

Dean G, Reubel G, Moore P, Pedersen N. Proviral burden and infection kinetics of feline immunodeficiency virus in lymphocyte subsets of blood and lymph node. J Virol. 1996; 70:5165–5169. [PubMed: 8764024]

Dianzani F, Antonelli G, Riva E, Uccini S, Visco G. Plasma HIV viremia and viral load in lymph nodes. Nat Med. 1996; 2:832–833. [PubMed: 8705839]

Dow SW, Dreitz KJ, Hoover EA. Feline immunodeficiency virus neurotropism: evidence that astrocytes and microglia are the primary target cells. Vet Immunol Immunopathol. 1992; 35:23–35. [PubMed: 1337399]

English RV, Johnson CM, Gebhard DH, Tompkins MB. In vivo lymphocyte tropism of feline immunodeficiency virus. J Virol. 1993; 67:5175–5186. [PubMed: 7688819]

Gray F, Lescs M-C, Keohane C, Paraire F, Marc B, Durigon M, Gherardi R. Early brain changes in HIV infection: neuropathological study of 11 HIV seropositive, non-AIDS cases. J Neuropathol Exp Neurol. 1992; 51:177–185. [PubMed: 1538241]

Gunn-Moore D, Pearson G, Harbour D, Whiting C. Encephalitis associated with giant cells in a cat with naturally occurring feline immunodeficiency virus infection demonstrated by in situ hybridization. Vet Pathol. 1996; 33:699–703. [PubMed: 8952030]

Harper ME, Marselle LM, Gallo RC, Wong-Staal F. Detection of lymphocytes expressing human T-lymphotropic virus type II in lymph nodes and peripheral blood from infected individuals by in situ hybridization. Proc Natl Acad Sci USA. 1986; 83:772–776. [PubMed: 3003749]

Hudson LC, Bragg DC, Tompkins MB, Meeker RB. Astrocytes and microglia differentially regulate trafficking of lymphocyte subsets across brain endothelial cells. Brain Res. 2005; 1058:148–160. [PubMed: 16137663]

Janeway, C.; Travers, P.; Walport, M.; Shlomchik, M. Immunobiology. Garland; New York: 2005.

Kim WK, Corey S, Chesney G, Knight H, Klumpp S, Wuthrich C, Letvin N, Koralnik I, Lackner A, Veasey R, Williams K. Identification of T lymphocytes in simian immunodeficiency virus encephalitis: distribution of CD8+ T cells in association with central nervous system vessels and virus. J Neurovirol. 2004; 10:315–325. [PubMed: 15385254]

Klevens RM, Fleming PL, Neal JJ, Li J. Is there really a heterosexual AIDS epidemic in the United States? Findings from a multisite validation study, 1992–1995. Mode of transmission validation study group. Am J Epidemiol. 1999; 149:75–84. [PubMed: 9883796]

Koenig S, Gendelman HE, Orenstein JM, Dal Canto MC, Pezeshkpour GH, Yungbluth M, Janotta F, Aksamit A, Martin MA, Fauci AS. Detection of AIDS virus in macrophages in brain tissue from AIDS patients with encephalopathy. Science. 1986; 233:1089–1093. [PubMed: 3016903]

Liu P, Hudson LC, Tompkins MB, Vahlenkamp TW, Colby B, Rundle C, Meeker RB. Cerebrospinal fluid is an efficient route for establishing brain infection with feline immunodeficiency virus and transferring infectious virus to the periphery. J Neurovirology. 2006a; 12:294–306. [PubMed: 16966220]

Liu P, Hudson LC, Tompkins MB, Vahlenkamp TW, Meeker RB. Compartmentalization and evolution of feline immunodeficiency virus between the central nervous system and periphery following intracerebroventricular or systemic inoculation. J Neurovirology. 2006b; 12:307–321. [PubMed: 16966221]

McGee B, Smith N, Aweeka F. HIV pharmacology: barriers to the eradication of HIV from the CNS. HIV Clin Trials. 2006; 7:142–153. [PubMed: 16880170]

Meeker R, Azuma Y, Bragg D, English R, Tompkins M. Microglial proliferation in cortical neural cultures exposed to feline immunodeficiency virus. J Neuroimmunol. 1999; 101:15–26. [PubMed: 10580809]

Nottet HS, Persidsky Y, Sasseville VG, Nukuna AN, Bock P, Zhai Q-H, Sharer LR, McComb RD, Swindells S, Soderland C, Gendelman HE. Mechanisms for the transendothelial migration of HIV-1-infection monocytes into brain. J Immunol. 1996; 156:1284–1295. [PubMed: 8558009]

Novotney C, English RV, Housman J, Davidson MG, Nasisse MP, Jeng C, Davis WC, Tompkins MB. Lymphocyte population changes in cats naturally infected with feline immunodeficiency virus. AIDS. 1990; 4:1213–1218. [PubMed: 1982410]

Pantaleo G, Graziosi C, Butini L, Pizzo PA, Schnittman SM, Kotler DP, Fauci AS. Lymphoid organs function as major reservoirs for human immunodeficiency virus. Proc Natl Acad Sci USA. 1991; 88:9838–9842. [PubMed: 1682922]

Pedersen N, Barlough J. Clinical overview of feline immunodeficiency virus. J Am Vet Med Assoc. 1991; 199:445–448.

Persidsky Y. Model systems for studies of leukocyte migration across the blood-brain barrier. J Neurovirol. 1999; 5:579–590. [PubMed: 10602399]

Persidsky Y, Stins M, Way D, Witte MH, Weinland M, Kim KS, Bock P, Gendelman HE, Fiala M. A model for monocyte migration through the blood-brain barrier during HIV-1 encephalitis. J Immunol. 1997; 158:3499–3510. [PubMed: 9120312]

Persidsky Y, Ghorade A, Rasmussen J, Limoges J, Liu X, Stins M, Fiala M, Way D, Kim K, Witte M, Weinland M, Carhart L, Gendelman H. Microglial and astrocyte chemokines regulate monocyte migration through the blood-brain barrier in human immunodeficiency virus-1 encephalitis. Am J Pathol. 1999; 155:1599–1611. [PubMed: 10550317]

Petito CK, Adkins B, McCarthy M, Roberts B, Khamis I. CD4+ and CD8+ cells accumulate in the brains of acquired immunodeficiency syndrome patients with human immunodeficiency virus encephalitis. J Neurovirol. 2003; 9:36–44. [PubMed: 12587067]

Quinn TC. The epidemiology of the acquired immunodeficiency syndrome in the 1990s. Emerg Med Clin North Am. 1995; 13:1–25. [PubMed: 7851311]

Roberts ES, Masliah E, Fox HS. CD163 identifies a unique population of ramified microglia in HIV encephalitis (HIVE). J Neuropathol Exp Neurol. 2004; 63:1255–1264. [PubMed: 15624762]

Ryan G, Klein D, Knapp E, Hosie MJ, Grimes T, Mabruk MJ, Jarrett O, Callanan JJ. Dynamics of viral and proviral loads of feline immunodeficiency virus within the feline central nervous system during the acute phase following intravenous infection. J Virol. 2003; 77:7477–7485. [PubMed: 12805447]

Sapatino BV, Welsh CJ, Smith CA, Bebo BF, Linthicum DS. Cloned mouse cerebrovascular endothelial cells that maintain their differentiation markers for factor VIII, low density lipoprotein and angiotensin-converting enzyme. In Vitro Cell Dev Biol. 1993; 29A:923–928.

Steffan A-M, Lafon M-E, Genrault J-L, Koehrin F, DeMonte M, Royer C, Kirn A, Gut J-P. Feline immunodeficiency virus can productively infect cultured endothelial cells from cat brain microvessels. J Gen Virol. 1994; 75:3647–3653. [PubMed: 7996160]

Strand OA. Acquired immunodeficiency syndrome (AIDS) in homosexual men—a new public health concern. NIPH Ann. 1982; 5:41–9. [PubMed: 6302568]

Wiley C, Schrier R, Nelson J, Lampert P, Oldstone M. Cellular localization of human immunodeficiency virus infection within the brain of acquired immune deficiency syndrome patients. Proc Natl Acad Sci USA. 1986; 83:7089–7093. [PubMed: 3018755]

Williams KC, Hickey WF. Central nervous system damage, monocytes and macrophages, and neurological disorders in AIDS. Annu Rev Neurosci. 2002; 25:537–562. [PubMed: 12052920]

Zheng J, Gendelman HE. The HIV-1 associated dementia complex: a metabolic encephalopathy fueled by viral replication in mononuclear phagocytes. Curr Opin Neurol. 1997; 10:319–325. [PubMed: 9266156]

Zink MC, Amedee AM, Mankowski JL, Craig L, Didier P, Carter DL, Munoz A, Murphey-Corb M, Clements JE. Pathogenesis of SIV encephalitis. Selection and replication of neurovirulent SIV. Am J Pathol. 1997; 151:793–803. [PubMed: 9284828]

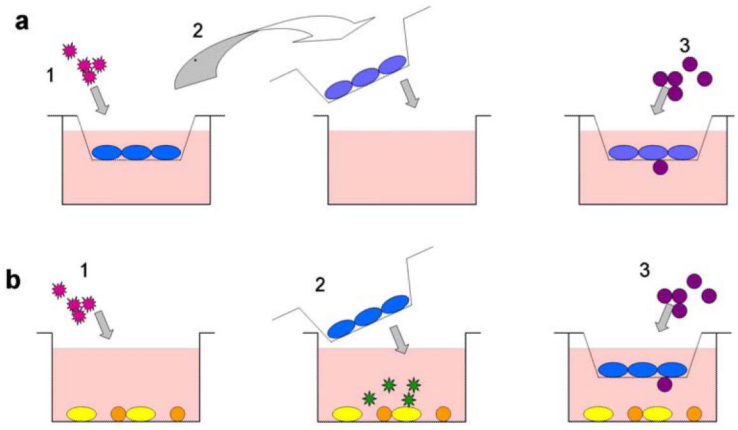

Fig. 1.

Representation of treatment protocol used for brain endothelial cells (BECs; **a**) and for astrocytes or microglia (**b**). **a***Step 1* Seeded BECs (day 1) were allowed to grow to confluence, and then virus was added to the upper chamber of the transwell insert for 24 h (day 3). *Step 2* The inserts were washed three times to remove any cell-free virus and subsequently moved to a fresh well with fresh medium in another plate. *Step 3* Treated peripheral blood mononuclear cells (PBMCs) were added to the upper chamber for 24 h (day 4). Adhered PBMCs and transmigrated PBMC subsets were measured (day 5). Controls included untreated PBMCs and untreated BECs and involved identical wash steps and transfer of inserts to fresh wells. **b** Two sets of plates with astrocytes, microglia, or both were prepared. In one plate, an insert with seeded BECs (day 1) was placed into the well, and BEC were allowed to grow to confluence under the influence of normal astrocytes and microglia. *Step 1* In the second plate, the astrocytes and/or microglia were seeded (day 1) and then treated with virus for 24 h (day 2). *Step 2* Astrocytes and microglia were washed three times to remove cell-free virus. The inserts with the confluent BECs were subsequently transferred from the untreated plate to the treated plate for 24 h (day 3). Factors (*green stars*) from treated astrocytes and/or microglia may effect BEC functions. *Step 3* Treated PBMCs were added to the upper chamber for 24 h (day 4). Adhered PBMCs and transmigrated PBMC subsets were measured (day 5). Controls included untreated PBMCs and untreated astrocytes and microglia and involved identical wash steps and transfer of inserts

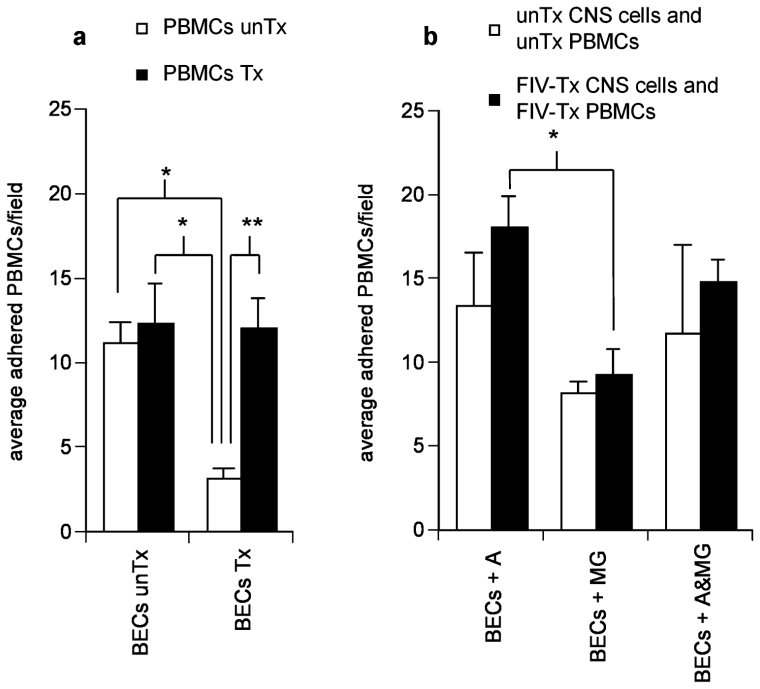

Fig. 2.

a, b Peripheral blood mononuclear cell (*PBMC*) adherence changes with PBMC and endothelial cell treatment (*Tx*) with FIV (*error bars* standard error of the mean, *P<0.05 for indicated pairs, **P<0.005 for indicated pair). **a** FIV treatment of brain endothelial cells (*BECs*) decreased adherence of PBMCs to the monolayer. FIV treatment of PBMCs returned adherence to levels seen with untreated (*unTx*) BECs and treated or untreated PBMCs. **b** PBMC adherence changes with PBMC and astrocyte (*A*) or microglia (*MG*) treatment with FIV. In configurations that included astrocytes or microglia, FIV treatment of PBMCs did not alter adherence levels compared with untreated PBMCs. Presence of astrocytes increased adherence of PBMCs to a BEC monolayer in comparison with the presence of FIV-treated microglia. When both astrocytes and microglia were present, the astrocyte effect appeared to be partially suppressed by the microglia

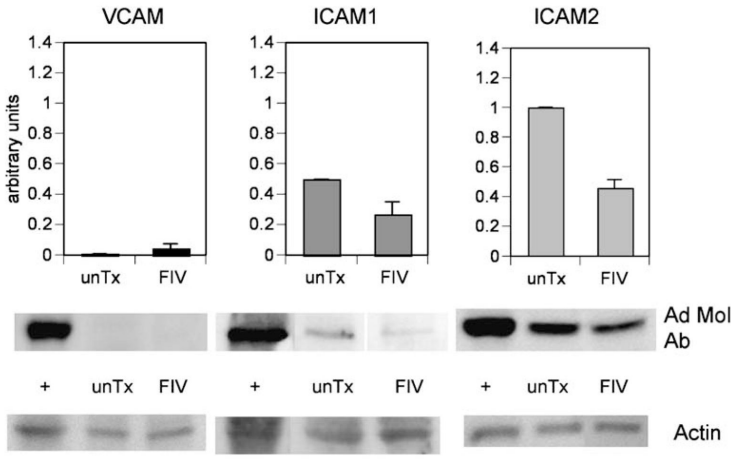

Fig. 3.

Acute (24 h) FIV exposure of BECs increased vascular cell adhesion molecule (*VCAM*) and decreased intracellular adhesion molecule 1 (*ICAM1*) and intracellular adhesion molecule 2 (*ICAM2*) expression on Western blot analysis compared with untreated cells (*unTx*). Data is representative of three independent experiments. The VCAM-positive control (+) was SOL8; the ICAM1-positive control (+) was HELA, and the ICAM2-positive control (+) was NAMALWA. Actin was used as a loading control, and densitometry values were normalized to actin control readings of untreated samples. VCAM demonstrated very low to absent constitutive expression, ICAM1 showed low constitutive expression, and ICAM2 showed robust constitutive expression. VCAM expression was increased after FIV exposure, but changes were not significant. ICAM1 and ICAM2 expression was decreased by approximately 50% upon acute FIV treatment of BECs (*Ad Mol Ab* antibody to each specific adhesion molecule)

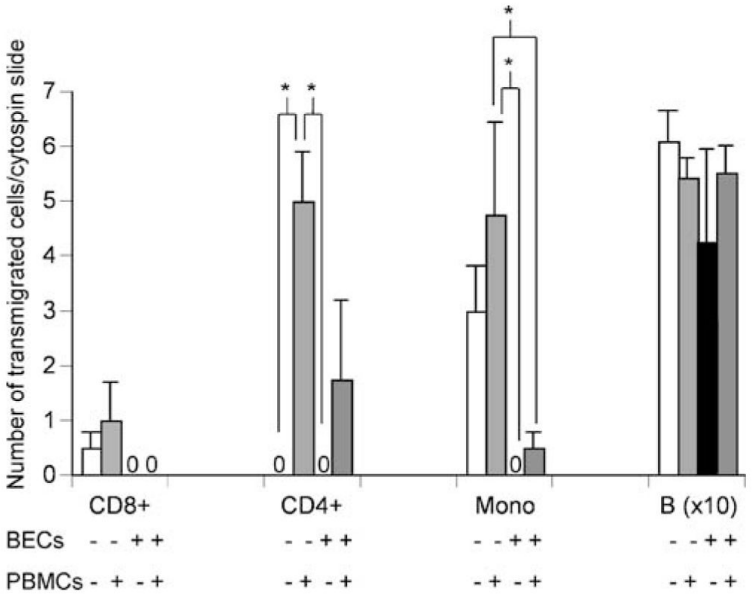

Fig. 4.

FIV treatment of PBMCs and of BECs differentially modulates transmigration of PBMC subsets (**P*<0.05 for indicated pairs, *error bars* standard error of the mean). BECs and PBMCs were present in all experiments and were either untreated with FIV (−) or treated with FIV for 24 h (+) and then cocultured for an additional 24 h. Transmigrated PBMCs were collected and stained for specific subsets. CD8 T cells (*CD8*+) overall had the lowest mean transmigration but the addition of FIV-treated PBMCs increased transmigration slightly. FIV treatment of BECs resulted in no transmigration of CD8 T cells. CD4 T cell (*CD4*+) transmigration was low when PBMCs were not FIV-treated but significantly increased with PBMC treatment and was decreased when BECs were FIV-treated. Similar to CD8 T cells, monocyte (*Mono*) transmigration was significantly decreased when BECs were FIV-treated. B cells (*B(×10)*) were the most extensively transmigrated cell of the various PBMC subsets studied. However, treatment of BECs and/or PBMCs with FIV did not alter the mean transmigration of this subset

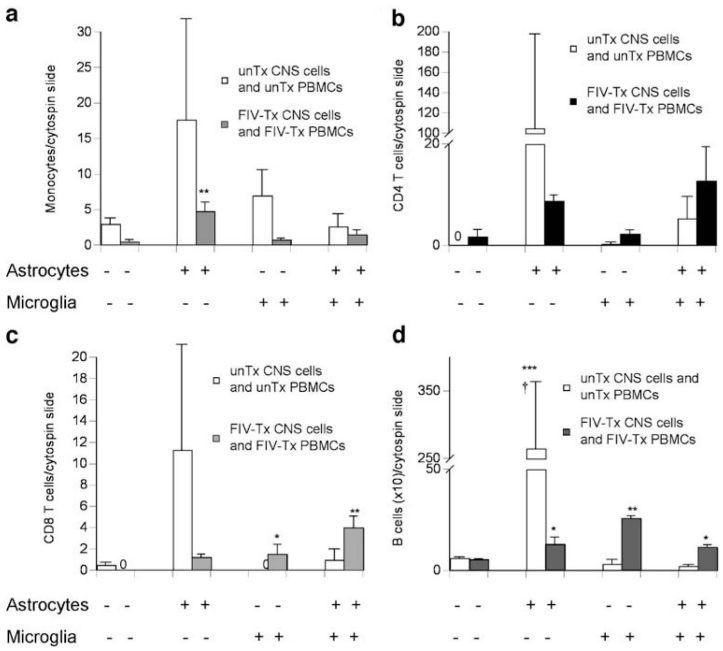

Fig. 5.

a–d FIV treatment of astrocytes, microglia and PBMCs differentially alters the transmigration of various PBMC subsets (*error bars* standard error of the mean). Astrocytes and/or microglia were present (+) or absent (−) in the configurations as indicated and were exposed to FIV for 24 h, before being co-cultured with BECs and untreated or FIV-treated PBMCs. **a** The presence of virus-treated astrocytes significantly increased mean monocyte transmigration by greater than two-fold (***P*<0.05) compared with other configurations of treated cells. Nevertheless, the mean transmigration of monocytes in the presence of FIV-treated cells was less than the mean transmigration in the presence of untreated cells. **b** In CD4 T cells, mean trafficking in the presence of FIV-treated cells increased with astrocytes or with astrocytes and microglia, but the observed variations precluded significant differences in transmigration numbers. **c** The presence of both FIV-treated astrocytes and microglia significantly increased transmigration of CD8 T cells (***P*<0.05) over the absence of astrocytes and microglia. Additionally, the presence of treated microglia only gave a significantly different result from that of the same configuration of cells without treatment (**P*<0.05). **d** B cell transmigration is increased with FIV-treatment of astrocytes and microglia. FIV-treated microglia exhibited an increase in transmigrated cells over treated configurations with astrocytes and microglia, astrocytes, or BECs only. Treated astrocytes or treated astrocytes and microglia demonstrated similar but smaller increases (**P*<0.05 over configuration with treated BECs only; ***P*<0.05 over all configurations with treated cells). In contrast, the configuration including untreated astrocytes was significantly increased over configurations with untreated microglia or both untreated astrocytes and microglia (****P*<0.05). BECs with untreated astrocytes and PBMCs was significantly increased over BECs with treated astrocytes and PBMCs (†*P*<0.001)

Table 1

Configuration of cells and treatment regimens (*X* cell type present in culture configuration, + cell type treated with FIV for 24 h, − cell type not treated with FIV)

PBMCs	BECs	Astrocytes	Microglia	Astrocytes and microglia	Replicates
X −	X−				*n*=5
X +	X −				*n*=6
X +	X +				*n*=6
X−	X +				*n*=5
X +	X −	X +			*n*=6
X +	X −		X +		*n*=6
X +	X −			X +	*n*=6
X−	X−	X−			*n*=5
X−	X−		X−		*n*=5
X−	X−			X−	*n*=5

Table 2

Immunocytochemistry and Western blot reagents (*HRP* horseradish peroxidase, *DAB* diaminobenzidine)

Primary antibody/source[a]	Dilution	Secondary biotinylated antibody/source	Avidin HRP	Substrate/source
Human ICAM1/Santa Cruz	1:100	Bovine anti-goat/HRP/ Santa Cruz		Chemiluminescence/Pierce
Human ICAM2/Santa Cruz	1:100	Goat anti-rabbit/HRP/Santa Cruz		Chemiluminescence/Pierce
Human VCAM/Santa Cruz	1:100	Bovine anti-goat/HRP/Santa Cruz		Chemiluminescence/Pierce
Actin/Santa Cruz	1:100	Bovine anti-goat/HRP/Santa Cruz		Chemiluminescence/Pierce
Feline CD4/Tompkins Lab	1:10	Mouse link/Biogenix	Biogenix kit	AEC/Biogenix
Feline CD8/Tompkins Lab	1:10	Mouse link/Biogenix	Biogenix kit	Vector SG/Vector Labs
Human CD3/DAKO	1:100	Mouse link/Biogenix	Biogenix kit	AEC/Biogenix
Feline B cell/Accurate	1:100	Link/Biogenix	Biogenix kit	DAB/Biogenix
Feline monocyte/Serotec	1:100	Mouse link/Biogenix	Biogenix kit	Vector SG/Vector Labs

[a]Santa Cruz Biotechnology, Santa Cruz, Calif.; Tompkins Lab (gift of Dr. Mary Tompkins, Raleigh, N.C.); DAKO, Carpentaria, Calif.; Accurate, Westbury, N.Y.; Serotec, Raleigh, N.C.; Biogenix, San Ramon, Calif.; Pierce Biotechnology, Rockford, Ill.; Vector Labs, Burlingame, Calif.